

SA-MixNet: Structure-aware Mixup and Invariance Learning for Scribble-supervised Road Extraction in Remote Sensing Images

Jie Feng^{1*} Hao Huang¹ Junpeng Zhang¹ Weisheng Dong¹ Dingwen Zhang² Licheng Jiao¹

¹Xidian University

jiefeng@xidian.edu.cn

²Northwestern Polytechnical University

Abstract

Mainstreamed weakly supervised road extractors rely on highly confident pseudo-labels propagated from scribbles, and their performance often degrades gradually as the image scenes tend various. We argue that such degradation is due to the poor model's invariance to scenes with different complexities, whereas existing solutions to this problem are commonly based on crafted priors that cannot be derived from scribbles. To eliminate the reliance on such priors, we propose a novel Structure-aware Mixup and Invariance Learning framework (SA-MixNet) for weakly supervised road extraction that improves the model invariance in a data-driven manner. Specifically, we design a structure-aware Mixup scheme to paste road regions from one image onto another for creating an image scene with increased complexity while preserving the road's structural integrity. Then an invariance regularization is imposed on the predictions of constructed and origin images to minimize their conflicts, which thus forces the model to behave consistently on various scenes. Moreover, a discriminator-based regularization is designed for enhancing the connectivity meanwhile preserving the structure of roads. Combining these designs, our framework demonstrates superior performance on the DeepGlobe, Wuhan, and Massachusetts datasets outperforming the state-of-the-art techniques by 1.47%, 2.12%, 4.09% respectively in IoU metrics, and showing its potential of plug-and-play. The code will be made publicly available.

1. Introduction

In recent years, remarkable performance improvement has been achieved in road extraction [10, 13, 23, 32], which partly relies on detailed annotations. In practical applications, it is challenging and costly to obtain such annotations,

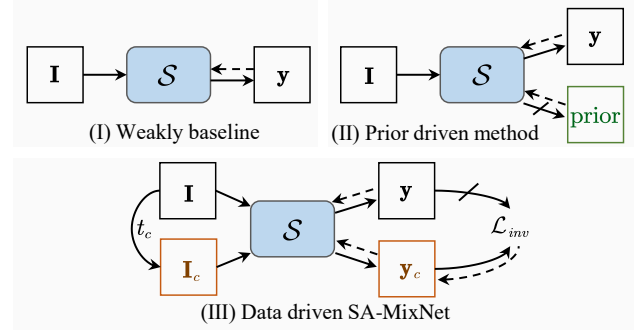


Figure 1. Overview of weakly supervised road extraction architectures: (I) Weakly supervised baseline with pseudo segmentation loss only, (II) Prior-driven method with additional manual prior, (III) Our proposed framework from data-driven manner without additional prior. Where t_c represents the sample construction. ‘ \rightarrow ’ means the forward operation. ‘ \dashrightarrow ’ means backpropagation. ‘ \nearrow ’ means stop-gradient. \mathcal{L}_{inv} means invariance regularization.

especially on large-scale remote sensing images. Therefore, learning with limited annotations has been emerging as a practical solution in such situations. Despite that point annotation has been continuously explored for weakly supervised road extraction [11], scribble is recognized as a better annotation form [25, 26, 34] as it provides additional clues on road structure.

In order to learn from scribbles, the expansion of highly confident supervision areas is key. Statistic-based methods [26, 34] employ a predefined width to expand the scribbles guided by statistic knowledge. However, a conservative width setting is necessary to avoid introducing incorrect information when dealing with significant variations in road widths, resulting in a lack of supervision. On a different front, methods focusing on image content [25] aim to reduce the reliance on statistics and handle the variety of road’s width, cluster similar pixel regions, and propagate labels by using image features [20]. Due to the sensitivity to

*Corresponding author: jiefeng@xidian.edu.cn

the initial clustering points, the clustering regions are difficult to adhere to rough road boundaries, which causes noisy annotations. In all cases, limitations and noise in annotations require additional regularized supervision to improve model generalization ability.

Some attempts have been made by introducing strong priors to the regularization learning process, shown in Fig. 1. Graph-based regularization methods [15, 22, 25, 26] are commonly used based on pixel similarity and structural priors, but they are sensitive to noise and high complexity in remote sensing images. On the other hand, collaborative learning-based regularization methods [25, 34] focus on road surface as well as additional edge or direction prior supervision, which can not be derived from weak labels. Additionally, existing methods’ performance commonly degrades as the samples tend to be complex in scenes of intertwined roads and indistinguishable backgrounds, leading to more missed detections in regions of confusion.

We argue that such degradation is due to the model’s poor invariance to road targets in scenes with different complexities. To address the above challenges, we proposed SA-MixNet, a novel Structure-aware Mixup and Invariance Learning framework for weakly supervised road extraction via scribble labels, shown in Fig. 1. First, we propose an improved mixup method, SA-Mixup, to operate on a pair of training samples by pasting one’s foreground regions onto the other. It constructs difficult samples with complex scenes while maintaining the road’s structural integrity. Then, to approach consistent performance on both constructed difficult and original samples, the invariance regularization is imposed on their predictions to minimize the conflict. It makes the model learn more robust and invariant foreground features by bridging the performance gap between difficult samples and general samples. Moreover, a topology regularization based on GAN is added to enhance the roads’ connectivity. To guarantee the performance of sample construction, a Statistic and Content-based Label Expansion (SCLE) is proposed to expand the highly confident foreground areas by taking road structure into specific consideration.

The main contributions of this paper are as follows:

1. We propose SA-MixNet, a novel framework for weakly supervised road extraction via scribble labels, that enhances the model’s generalization ability from a data-driven perspective and eliminates the requirements for additional priors.
2. The proposed structure-aware Mixup constructs proper scenes with various complexities for the invariance learning framework while mitigating road sample imbalance and maintaining the road’s structural integrity.
3. The invariance regularization is proposed to force the model to approach consistent performance on original and constructed samples. It guarantees the model’s in-

variance under different conditions, resulting in a profound performance improvement on ambiguity samples.

4. Experiments on three datasets *i.e.* DeepGlobe, Wuhan, and Massachusetts-road, show that SA-MixNet achieves the best performance on the weakly supervised road extraction, and shows the potential of its plug-and-play to be used to improve the performance of other existing methods.

2. Related Works

2.1. Weakly Supervised Road Extraction

In road extraction from remote sensing images, imbalanced sample distribution and undistinguishable roads from background often lead to broken connections and incomplete structures, especially in complex scenes. Such difficulties tend more severe under limited annotations. Existing weakly supervised methods attempt to mitigate this issue by focusing on pseudo-label generation and regularization learning.

In the label generation phase, statistics-based methods [26, 34] can simply and effectively extend scribbles but may struggle to accommodate roads of varying widths. Wei et al.[25] used SLIC [1] clustering to combine statistical and image features, reducing reliance on statistical knowledge. However, SLIC’s sensitivity to initial points leads to noisy annotations to road boundaries.

Learning from such limited annotations with noise requires additional regularization supervision to enhance the model’s generalization performance. Some methods provide extra supervision based on graph optimization [15, 22, 25, 26] through pixel similarity and structural priors, but they are susceptible to inherent noise in remote sensing images and perform poorly in complex scenes, affecting the model’s generalization. Other methods use multi-branch networks [25, 34] to extract road surface in a collaborative learning manner, but they typically require additional edge or direction prior supervision that cannot be derived from scribbles.

2.2. Mixup Strategies

The addition of perturbation on input-level [17, 19, 21, 31], feature-level [16, 18, 27] or both [9, 17] has been used in semi-supervised and self-supervised learning to generalize models with limited data. Input-level perturbation improves the robustness and generalizability of both encoders and decoders by utilizing unlabeled data efficiently. Its simplicity and transferability have contributed to its broad application. Recently, mixup techniques stand out as an effective method for implementing input-level perturbation.

Rooted in data augmentation basics like rotation, cropping, flipping, and color jittering, non-heuristic Mixup [29]

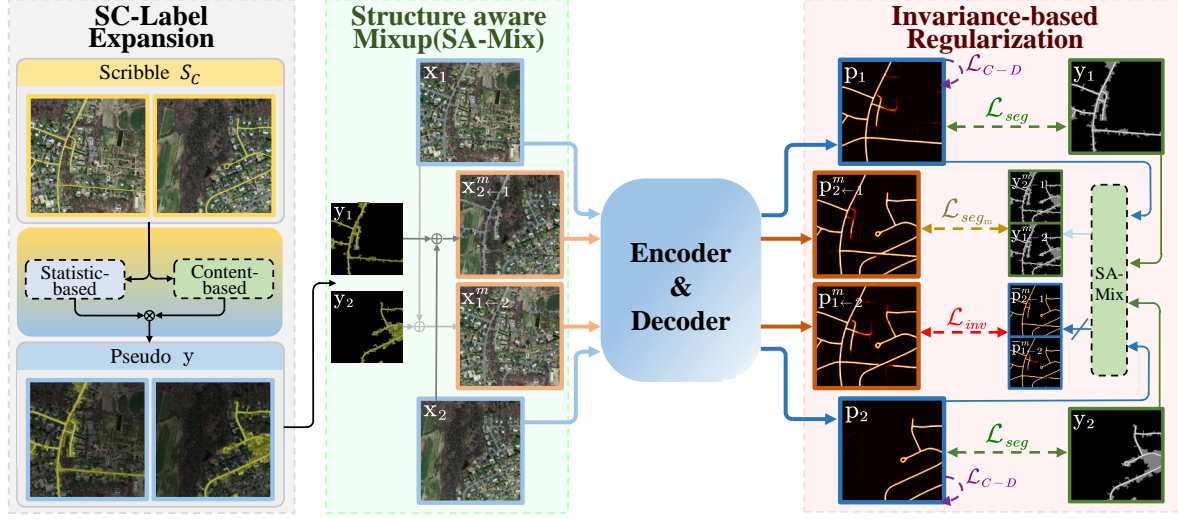


Figure 2. The pipeline of proposed SA-MixNet, consisting of three parts: Statistic and Content-based (SC) Label Expansion, Structure-aware Mixup (SA-Mix) based sample construction, and Invariance-based Regularization including base segmentation loss (\mathcal{L}_{seg} & \mathcal{L}_{seg_m}), invariance regularization (\mathcal{L}_{inv}), and the connectivity regularization (\mathcal{L}_{C-D}). ‘/’ on ‘ \rightarrow ’ means stop-gradient.

blends the images and labels by pixel-wise linear addition to craft new examples, improving model performance with subtle data variations. Other non-heuristic methods like CutMix[28] and FMix[5] randomly generate rectangular or smooth masks for pasting and covering between samples. Building on this, heuristic methods such as Co-Mixup[8] and PuzzleMix [7] preserve areas of high responsiveness during pasting based on the strength of gradients from back-propagation.

For road targets, most of the existing mixup methods select partial image blocks for pasting without considering the grid-like characteristics and spanning nature of road objects in remote sensing images, bringing damage to roads’ structure integrity.

3. Methodology

3.1. Overview of SA-MixNet

The proposed SA-MixNet presents a unified weakly supervised framework for road extraction using scribble labels. As illustrated in Fig. 2, it includes the basic statistic and content-based label expansion, structure-aware Mixup module, and invariance regularization. The label propagation first updates the scribble labels with statistic information, and refined statistic-based pseudo label by incorporating road-specific content-based clustering into statistic-based expansion. Then, structure-aware Mixup module is proposed by pasting the generated roads and buffers randomly to construct new image scenes with various complexities. Finally, the invariance regularization is imposed to force the model to approach consistent perfor-

mance on original and constructed samples. Moreover, a discriminator-based regularization is added for enhancing the connectivity meanwhile preserving the structure of the road.

3.2. Statistic and Content-based Label Expansion

The scribble annotation is easily accessible, but it rarely provides sufficient supervising information. The intuitive method is to expand the scribble annotation with width statistic information, but it may lead to poor adaptability on roads with various widths. To improve the label expansion, we incorporate road-specific content-based clustering into statistic-based expansion, as illustrated in Fig.3.

Statistic-based Label Expansion According to the statistical knowledge of road width, b_1 and b_2 are chosen as the upper and lower limits of roads to perform the buffer expansion, respectively. The statistic-based pseudo labels y_s^i of the pixels p_i is classified as

$$y_s^i = \begin{cases} 1 & (\text{foreground}) \quad \text{if } 0 < \text{DIS}_{p_i} \leq b_1, \\ 0.5 & (\text{uncertain}) \quad \text{if } b_1 < \text{DIS}_{p_i} \leq b_2, \\ 0 & (\text{background}) \quad \text{if } \text{DIS}_{p_i} > b_2, \end{cases} \quad (1)$$

where DIS_{p_i} denotes the distance from the pixel p_i to the scribble. $y_s^i \in \{1, 0, 0.5\}$ is the statistic-based label of the pixel p_i , which represents the class of *foreground*, *background*, and *uncertain* region, respectively.

Road-specific Content-based Clustering Clustering-based method [1, 25] improves the efficiency and explores

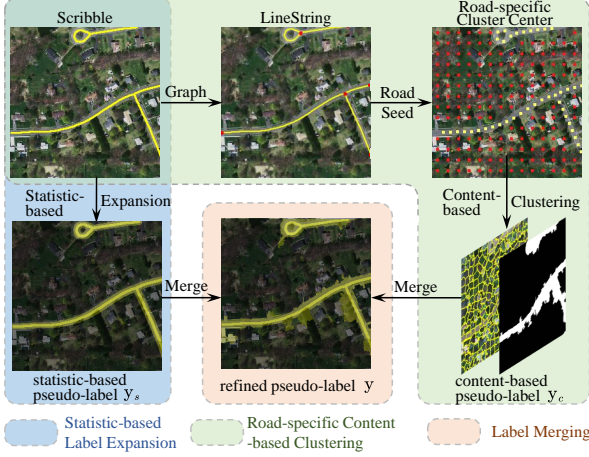


Figure 3. The flow chart of Statistic and Content-based Label Propagation, including statistic-based expansion (annotated with blue), content-based clustering (annotated with green), and the merge of statistic-based pseudo label y_s and content-based pseudo label y_c (annotated with orange).

similar pixels by grouping the pixels into meaningful regions. We further improve upon this method by using road-specific seed points as initial clustering centers, alleviating the issues caused by cluster’s sensitivity to initial points and enhancing adherence to rough road boundaries.

For scribble labels, we select intersections and start/end points as key points d_{key} , and perform sampling with a stride of q on each scribble to obtain representative points d_{rep} . Both d_{key} and d_{rep} collectively serve as foreground seeds. q is calculated as

$$q = \frac{H \cdot W}{\sqrt{2} \cdot \sqrt{N_{SLIC}}}, \quad (2)$$

where N_{SLIC} is the number of superpixels and $(H \times W)$ is the resolution of the image. Background seeds are sampled at intervals of $H \cdot W / N_{SLIC}$. Seeds within $(b_1 + b_2)/2$ pixels of the scribbles are discarded to prevent interference with road areas. We then use Graph Cut [22] to categorize superpixels into *background* and *foreground* with potential road regions, generating content-based pseudo labels $y_c^i \in \{0, 1\}$.

Label Merging The statistic-based label expansion hardly provides the buffer areas that adapt to different roads, it may lead to a potential category conflict between y_c and y_s . Thus, the buffer setting is refined based on the content-based pseudo labels. The refined pseudo labels y^i are defined as

$$y^i = \begin{cases} 0.5 \text{ (uncertain)} & \text{if } y_s^i = 0 \text{ and } y_c^i = 1, \\ y_s^i & \text{otherwise.} \end{cases} \quad (3)$$

In Eq. (3), if the pixel p_i is identified as *background* by statistic-based expansion and as *foreground* by content-based expansion, it will be updated as *uncertain* buffer. Otherwise, keep the statistic-based label y_s^i unchanged.

3.3. Structure-aware Mixup

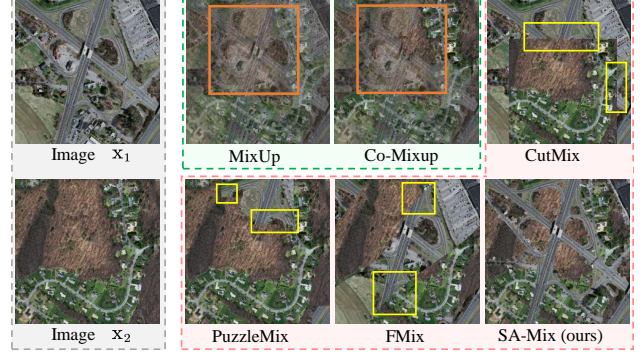


Figure 4. The visualization of different *mixup* methods. Methods causing image overlay are green, and the indistinguishable regions are marked by the orange box; Non-overlay methods are red, and the damaged structures are marked by the yellow box. Our proposed SA-Mix has better road structure integrity compared to other methods, generating samples with proper scenes.

Most existing mixup methods use block-based pasting while leaving the structural characteristics of the roads unconsidered, which thus risks generating impractical images, shown in Fig. 4. In order to construct samples with more complex image scenes, we propose a novel perturbation scheme to paste foreground regions with an explicit focus on roads’ structure, namely structure-aware Mixup (SA-Mix). It constructs the images by significantly increasing the variety of road intersections and diverse combinations of foreground and background.

For a given pair of images (x_1, x_2) , SA-Mix takes the refined pseudo label (y_1, y_2) as a structural clue, and pastes the non-background regions onto the other image. The constructed images $(x_{1 \leftarrow 2}^m, x_{2 \leftarrow 1}^m)$ representing paste x_2 to x_1 and x_1 to x_2 respectively are obtained as

$$\begin{cases} x_{1 \leftarrow 2}^m = D_{KL}(x_1, x_2) \cdot [x_1 \odot (1 - \alpha_2) + x_2 \odot \alpha_2] \\ \quad + [1 - D_{KL}(x_1, x_2)] \cdot x_1, \\ x_{2 \leftarrow 1}^m = D_{KL}(x_1, x_2) \cdot [x_2 \odot (1 - \alpha_1) + x_1 \odot \alpha_1] \\ \quad + [1 - D_{KL}(x_1, x_2)] \cdot x_2, \end{cases} \quad (4)$$

where \odot refers to the element-wise multiplication, and $\alpha_i = \mathbf{I}(y_i > 0)$ is the mask of non-background regions in y_i generated by the indicator function $\mathbf{I}(\cdot)$.

For preventing interfering edges on a pair of images with significant color differences, we introduce a binary indicator $D_{KL}(x_1, x_2)$ based on the color similarity between the

image pair in HSV space, defined as

$$D_{KL}(\mathbf{x}_1, \mathbf{x}_2) = \begin{cases} 1 & \text{if } \mathbf{KLDiv}(\text{Hist}_1, \text{Hist}_2) < t, \\ 0 & \text{otherwise,} \end{cases} \quad (5)$$

where $\mathbf{KLDiv}(\cdot, \cdot)$ denotes the Kullback–Leibler (KL) divergence. t is a threshold for filtering out the image pairs with extreme color differences, such that interfering edges can be properly suppressed.

For the filtered image pair, a similar mixing operator is applied on their pseudo labels, and the pseudo labels for the constructed images ($\mathbf{y}_{1 \leftarrow 2}^m, \mathbf{y}_{2 \leftarrow 1}^m$) are obtained as

$$\begin{aligned} \mathbf{y}_{1 \leftarrow 2}^m &= \mathbf{y}_1 \odot (1 - \alpha_2) + \mathbf{y}_2 \odot \alpha_2, \\ \mathbf{y}_{2 \leftarrow 1}^m &= \mathbf{y}_2 \odot (1 - \alpha_1) + \mathbf{y}_1 \odot \alpha_1. \end{aligned} \quad (6)$$

3.4. Supervision of SA-MixNet

In our SA-MixNet, the training process is jointly optimized by segmentation loss, invariance regularization, and connectivity regularization. Along with such basic pseudo segmentation supervision, we propose invariance regularization (\mathcal{L}_{inv}) to force the model to approach consistent performance on original and constructed samples, enhancing the model’s invariance under different conditions. Moreover, discriminator-based connectivity regularization (\mathcal{L}_{C-D}) is designed to improve the topology connectivity of roads. The overall loss \mathcal{L} can be summarized as

$$\mathcal{L} = \mathcal{L}_{seg} + \mathcal{L}_{seg_m} + \lambda_1 \mathcal{L}_{inv} + \lambda_2 \mathcal{L}_{C-D}, \quad (7)$$

where, the contribution of these loss terms to the overall training loss is controlled by their corresponding coefficients λ_1, λ_2 .

\mathcal{L}_{seg} and \mathcal{L}_{seg_m} are the segmentation losses designed to minimize the differences between predictions (\mathbf{p}) and pseudo labels (\mathbf{y}) on both original and constructed samples, defined as

$$\begin{aligned} \mathcal{L}_{seg} &= \frac{1}{2} [\mathcal{L}_p(\mathbf{y}_1, \mathbf{p}_1) + \mathcal{L}_p(\mathbf{y}_2, \mathbf{p}_2)], \\ \mathcal{L}_{seg_m} &= \frac{1}{2} [\mathcal{L}_p(\mathbf{y}_{1 \leftarrow 2}^m, \mathbf{p}_{1 \leftarrow 2}^m) + \mathcal{L}_p(\mathbf{y}_{2 \leftarrow 1}^m, \mathbf{p}_{2 \leftarrow 1}^m)], \end{aligned} \quad (8)$$

where $\mathcal{L}_p(\cdot, \cdot)$ represents Partial BCE loss that measures Cross-Entropy on foreground and background pixels while ignoring those *uncertain* ones.

Invariance Regularization Actually, the samples constructed by SA-Mixup are more challenging than the original ones by adding extra road intersections and combinations of backgrounds and foregrounds. In order to ensure that the model has sustained outstanding performance in dealing with such challenging samples, directed invariance regularization is designed. It is inspired by consistency

learning, and it improves the model’s learning ability for difficult samples by forcing the model to perform as well on the constructed samples as the original ones.

The expected invariance between predictions of constructed samples \mathbf{p}^m and mixed original predictions $\bar{\mathbf{p}}^m$ are formulated as

$$\begin{aligned} \mathcal{S}(\text{SA-Mix}(\mathbf{x}_1, \mathbf{x}_2)) &= \text{SA-Mix}(\mathcal{S}(\mathbf{x}_1), \mathcal{S}(\mathbf{x}_2)), \\ \mathbf{p}_{1 \leftarrow 2}^m, \mathbf{p}_{2 \leftarrow 1}^m &= \bar{\mathbf{p}}_{1 \leftarrow 2}^m, \bar{\mathbf{p}}_{2 \leftarrow 1}^m, \end{aligned} \quad (9)$$

where $\mathcal{S}(\cdot)$ represents the segment method, and \mathcal{L}_{inv} is defined based on cosine similarity \mathcal{L}_{cos} as

$$\begin{aligned} \mathcal{L}_{inv} &= \frac{1}{2} [\mathcal{L}_{cos}(\mathbf{p}_{1 \leftarrow 2}^m, \bar{\mathbf{p}}_{1 \leftarrow 2}^m) + \mathcal{L}_{cos}(\mathbf{p}_{2 \leftarrow 1}^m, \bar{\mathbf{p}}_{2 \leftarrow 1}^m)], \\ \mathcal{L}_{cos}(\mathbf{p}^m, \bar{\mathbf{p}}^m) &= 1 - \frac{\mathbf{p}^m \cdot \bar{\mathbf{p}}^m}{\|\mathbf{p}^m\| \cdot \|\bar{\mathbf{p}}^m\|}, \end{aligned} \quad (10)$$

where \perp is an operator that sets the gradient of the operand to zero. Consequently, the gradient of \mathcal{L}_{inv} is truncated at the prediction of the original image and directed backpropagated to the constructed image.

Connectivity Regularization The connectivity regularization is designed to enhance the connectivity integrity of roads through adversarial learning without introducing additional supervising information. It is applied to original images’ predictions.

Utilizing the encoder-decoder module as the generator, we incorporate a topological connectivity network inspired by patch GAN [35] as the discriminator. The detailed architecture is shown in the Fig. 5

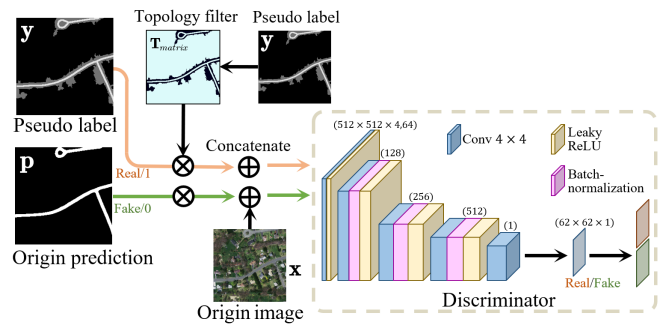


Figure 5. The pipeline of topological connectivity discriminator. The *Pseudo label* \mathbf{y} and *Prediction* \mathbf{p} are filtered by the *Topology filter* \mathbf{T}_{matrix} generated by the *Pseudo label* \mathbf{y} , then concatenated with *Image* \mathbf{x} respectively, and input into the *Discriminator*.

First, we generate a topological filter matrix \mathbf{T}_{matrix} based on \mathbf{y} , which is used to extract topological connectivity features and determined background features ignoring edge information in the *uncertain* region of \mathbf{p} and \mathbf{y} . The

process is defined as

$$\mathbf{p}_T, \mathbf{y}_T = \mathbf{p} \odot \mathbf{T}_{matrix}, \mathbf{y} \odot \mathbf{T}_{matrix}, \quad (11)$$

where

$$\mathbf{T}_{matrix} = \begin{cases} 1 & \text{if } \mathbf{y} = 1 \text{ or } \mathbf{y} = 0, \\ 0 & \text{if } \mathbf{y} = 0.5. \end{cases} \quad (12)$$

Then \mathbf{p}_T and \mathbf{y}_T are concatenated with images \mathbf{x} to get \mathbf{x}_d as input of the discriminator (\mathcal{D}). \mathcal{D} outputs an evaluation vector of size $N \times N \times 1$ to assess the topological integrity of roads and less false detection in each region. The cross-entropy loss is calculated for the true and false classes as

$$\begin{aligned} \mathcal{L}_{C-D} = & - \sum_{h,w} (1 - y_n) \log(\mathcal{D}(\mathbf{x}_d)^{(h,w,0)}) \\ & + y_n \log(\mathcal{D}(\mathbf{x}_d)^{(h,w,1)}). \end{aligned} \quad (13)$$

It forces the model to make predictions with less false detection and better connectivity.

4. Experiment and Results

4.1. Datasets and Implementation

Datasets We evaluate the proposed SA-MixNet on three challenging datasets, *i.e.* DeepGlobe, Massachusetts-road, and Wuhan. These datasets cover a variety of scenes, including urban, rural and suburban areas.

DeepGlobe [4] is one of the largest datasets of road extraction. It contains 6226 images in size of 1024×1024 , and the ground resolution of each image is 50cm/pixel. Following [2, 3], the entire dataset is split into 4696 and 1530 images for training and testing, respectively.

Massachusetts-road [14] contains 1108 images, 14 images, and 49 images for training, validation, and testing. These images are with a pixel resolution of 1500×1500 , their ground resolution is 1.2m/pixel. The road widths in this dataset are mostly consistent.

Wuhan is another dataset for road extraction containing 2592 images in size of 1024×1024 and a ground resolution of 50cm/pixel. The road widths in this dataset vary significantly. Following [25], we create two splits with 1944 images and 648 images for training and testing, respectively.

While these datasets contain fully annotated road masks, the scribble labels are generated by skeletonizing the road masks. Non-overlapping cropping is performed on DeepGlobe and Wuhan datasets, resulting in 18784 training and 6120 testing samples of 512×512 for DeepGlobe dataset, 7776 training and 2592 testing samples of 512×512 for Wuhan dataset. For Massachusetts-road, overlapping cropping is performed to get 9972, 126, and 441 samples for training, validation, and testing, respectively.

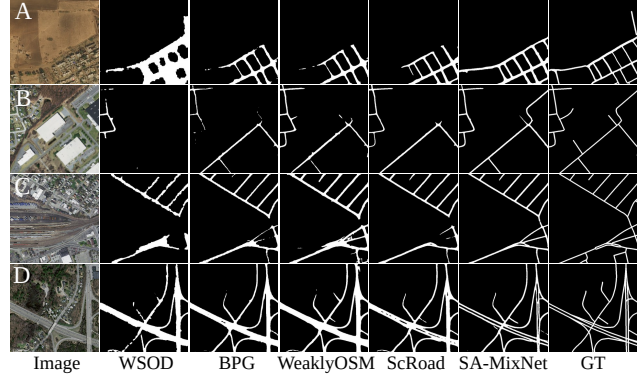


Figure 6. Visualization of GT, and WSOD, BPG, WeaklyOSM, ScRoadExtractor, SA-MixNet(ours)’s predictions of selected images with complex scenes. A) roads sharing similar features with background, B) blurry road areas, C) railways resembling road features, and D) overpasses with complex intersections

Implementation Details Our SA-MixNet is based on D-LinkNet [33] with a ResNet-34 backbone. We employ the Adam optimizer to refine both the D-LinkNet and the discriminator. The initial learning rates are set to 2×10^{-4} for D-LinkNet and halved for the discriminator. The learning rates are decayed with a rate of 0.2 when the loss does not decrease for 6 epochs. Early stopping is triggered when the loss remains unchanged for 12 epochs. During training, image flipping, rotation, mirroring and color shifts are adopted for data augmentation. Our model is trained with a batch size of 16. For pseudo-label propagation, we adopt the same buffer zone setting as [25].

4.2. Main Results

Comparison with Weakly Supervised Methods Tab. 1 summarizes the evaluation metrics by the proposed SA-MixNet on DeepGlobe, Wuhan and Massachusetts-Road datasets.

Compared against weakly supervised methods via scribble labels, the proposed SA-MixNet achieves the highest scores on these datasets in terms of IoU and F1 scores. It achieves IoU gains of 1.47%, 2.12% and 4.09% against current best performer ScRoadExtractor with an edge detection branch supervised by additional boundaries data on the DeepGlobe, Wuhan and Massachusetts-road datasets, respectively. Surprisingly, SA-MixNet with the basic ResNet-34 backbone outperforms BPG with stronger DeepLabV2-101 backbone.

For qualitative evaluation, a set of complex scenes are selected, including roads sharing similar features with background, blurry road areas, railways resembling road features, and overpasses with complex intersections. As visualized in Fig. 6, our SA-MixNet outperforms other methods in adapting to diverse scenarios. It delivers better edge

		DeepGlobe				Wuhan				Massachusetts-road			
Method	Description	IoU	F1	Precision	Recall	IoU	F1	Precision	Recall	IoU	F1	Precision	Recall
ScribbleSup[12]	VGG-16	26.94	40.79	29.51	88.13	47.40	62.22	60.86	72.67	—	—	—	—
WSOD[30]	VGG-16	46.87	63.82	59.96	68.21	48.87	65.66	64.09	67.31	42.04	59.20	62.96	55.85
BPG[24]	DeepLabV2-101	54.00	70.13	66.90	73.68	50.86	67.43	76.66	60.19	55.45	71.34	66.32	77.18
MixUp[29]		51.02	67.57	55.52	86.31	51.97	68.39	79.54	59.99	60.58	75.45	70.50	81.14
Co-Mixup[8]	+ D-LinkNet-34	52.78	69.10	85.08	58.18	52.71	69.03	78.68	61.49	60.67	75.52	75.63	75.42
FMix[5]	+ proposed \mathbf{y}	57.57	73.07	75.04	71.21	53.73	69.90	75.00	65.45	60.81	72.63	72.96	78.50
CutMix[28]	+ proposed \mathcal{L}	58.28	73.64	74.73	72.59	52.93	69.22	70.89	67.63	61.45	76.12	73.30	79.18
PuzzleMix[7]		58.79	74.05	72.05	76.16	54.87	70.86	75.36	66.86	62.25	76.73	74.88	78.68
Baseline _{weak}	D-LinkNet-34	57.00	72.61	72.88	72.35	52.56	68.91	67.65	70.22	55.34	71.25	62.43	82.98
WeaklyOSM[6]	MD-ResUnet	54.32	70.40	68.85	72.03	52.34	68.72	67.93	69.52	52.74	69.06	57.83	85.67
ScRoad[26]	DBNet-34	58.91	74.14	70.79	77.82	53.64	69.82	75.29	65.10	58.19	73.57	67.89	80.28
SA-MixNet (ours)	D-LinkNet-34	60.38	75.29	73.30	77.40	55.76	71.59	74.06	69.29	62.28	76.77	73.66	80.13

Table 1. Comparison of the proposed method against state-of-the-art generic, road-specific weakly supervised techniques and various strong mixup methods incorporating the proposed SA-MixNet framework on the DeepGlobe, Wuhan, and Massachusetts-road datasets.

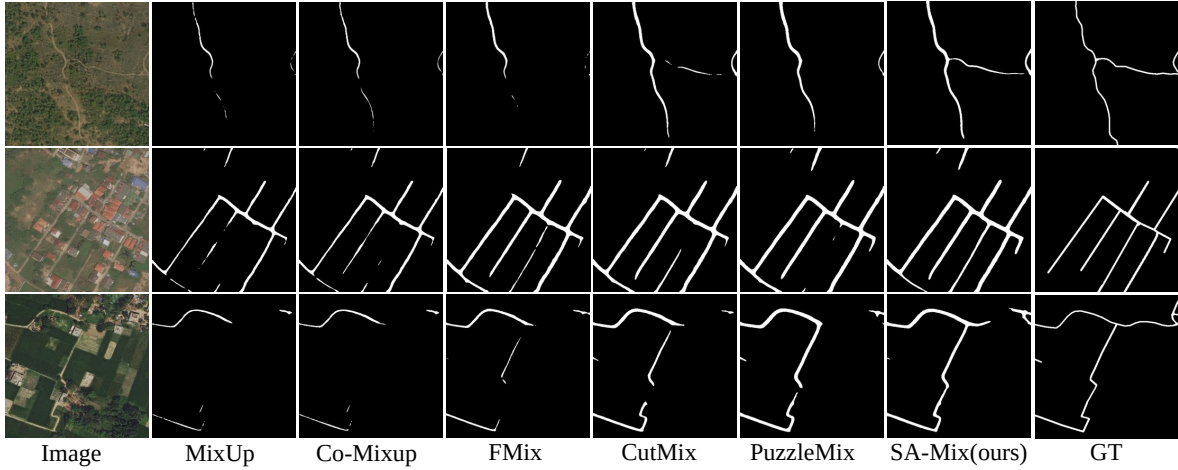


Figure 7. Visualization of MixUp, Co-Mixup, FMix, CutMix, PuzzleMix, and our SA-Mix’s predictions. All mentioned *mixup* methods use pseudo labels generated by our proposed SC-label expansion, and are supervised by proposed invariance-based regularization \mathcal{L} .

and road structure than BPG and ScRoadExtractor where an extra boundary detection branch is deployed, even under conditions of similar features, unclear edges and pixel blurriness. Such improvement demonstrates that our SA-MixNet is capable of extracting road features with remarkable invariance across diverse scenes. Moreover, the road masks predicted by our SA-MixNet also exhibit better road connectivity than other methods. This may partly be attributed to the connectivity regularization during model training, and further analyses will be conducted in subsequent Sec. 4.3.

Comparison with Mix-up Method To verify the effectiveness of our proposed SA-Mix module, we replaced it with various strong mixup schemes [5, 7, 8, 28, 29]. For a fair comparison, the identical segmentor and pseudo-label

generation strategy to our SA-MixNet are adopted for these methods, as well as the same learning framework.

As summarized in Tab. 1 the proposed SA-Mix outperforms the best-listed PuzzleMix method by 1.59%, 0.89% on DeepGlobe and Wuhan dataset in terms of the IoU metric. Remote sensing imagery encapsulates a higher level of complexity and intricacy compared to standard natural images. Such complexity renders techniques like Mixup and Co-Mixup less effective due to issues of overlapping. As visualized in Fig. 7, Mixup and Co-Mixup achieve inferior predictive performance, as the indistinguishability caused by overlapping impedes their ability to accurately capture features. The predicted road masks by non-heuristic methods, FMix and CutMix, suffer from severe fragmentation because the topological structure of roads is not considered. The heuristic PuzzleMix method is capable of preserving

road structures to a certain extent during the patching process. Unlike the above mixup schemes, our proposed SA-Mix method achieves the best performance in maintaining topological integrity, signifying its superior capability in preserving the continuity of road topology.

4.3. Ablation Study

In this section, we examine the contribution of segmentation loss, invariance regularization and connectivity regularization to the superior performance improvement by our SA-MixNet.

Loss				DeepGlobe			
\mathcal{L}_{seg}	\mathcal{L}_{seg_m}	\mathcal{L}_{inv}	\mathcal{L}_{C-D}	IoU	F1	Precision	Recall
✓				58.81	74.07	75.17	73.00
✓	✓			59.34	74.48	73.48	74.48
✓	✓	✓		60.09	75.07	72.43	77.91
✓	✓	✓	✓	60.38	75.29	73.30	77.40

Table 2. Ablation study of loss design on DeepGlobe dataset

Our baseline model only adopts the segmentation loss \mathcal{L}_{seg} for supervision. As summarized in Tab. 2, the introduction of SA-Mixup for sample construction, supervised by \mathcal{L}_{seg_m} , leads to an IoU gain of 0.53%. This highlights the positive impact of a more diverse and challenging set of learning samples on model efficacy.

Additionally, activating the proposed invariance regularization yields a further IoU improvement of 0.75%. This validates that, by forcing the model to align its performance on constructed samples with that on original ones, this invariance regularization helps identify ambiguous samples. Along with the improvement on IoU scores, the recall rate is also increased by adopting \mathcal{L}_{seg_m} and \mathcal{L}_{inv} . This validates that \mathcal{L}_{seg_m} and \mathcal{L}_{inv} help enhance the model’s ability to recognize road features. With a significant increase of 3.43% in recall rates, \mathcal{L}_{inv} is believed to play a more important role in enhancing the model’s invariance across various scenes.

Furthermore, by introducing \mathcal{L}_{C-D} , an additional 0.29% improvement in IoU score is achieved. This highlights its role in reducing false positives and enhancing connectivity.

4.4. Data Sensitivity Study

We investigated the annotation sensitivity of the proposed SA-MixNet with varying ratios of scribble to full annotations on DeepGlobe dataset.

As shown in Tab. 3, our SA-MixNet, with 100% scribble annotations, surpasses the baseline (D-LinkNet) by 3.38% in IoU. The IoU score gradually increases, as more full annotations are fed for training. It tends stable after the portion of full annotation reaches 50%. Noteworthily, our method’s IoU outperforms the fully supervised benchmark with just 25% full annotations, and, with complete annotations, it exceeds this benchmark by 3.15%. These results imply that

Weak : Full	IoU	F1	Precision	Recall
100% : 0%	60.38	75.29	73.30	77.40
90% : 10%	63.18	77.44	75.29	79.71
75% : 25%	65.87	79.42	78.12	80.76
50% : 50%	67.06	80.28	78.44	82.22
25% : 75%	67.69	80.73	79.81	81.68
0% : 100%	68.10	81.02	79.52	82.58
D-LinkNet _w	57.00	72.61	72.88	72.35
D-LinkNet _f	64.95	78.75	81.44	76.23

Table 3. Data sensitive study on DeepGlobe dataset

SA-MixNet, with a few increase in full annotations, can markedly enhance performance at various annotation levels and it is also highly effective under fully supervised conditions.

4.5. Generalizability on Different Road Extractors

To further validate the generalizability of our proposed framework, SA-MixNet, across different models, we replace the encoder-decoder network with ScRoadExtractor’s dual-branch network (DBNet)[25] and compare the performance with origin DBNet on DeepGlobe dataset. The pseudo labels generated by our SC-label expansion are applied.

Method	DBNet _{w/edge}		Ours + DBNet _{wo/edge}		Ours + DBNet _{w/edge}	
dataset	IoU	F1	IoU	F1	IoU	F1
DeepGlobe	59.48	74.14	60.56	75.43	60.50	75.39
Wuhan	54.45	70.50	55.38	71.28	54.45	70.51
Ma	59.47	74.59	62.60	77.00	62.36	76.81

Table 4. Generalizability Experiment

As shown in Tab. 4, after integrating with the proposed framework to DBNet without the edge detection branch, the IoU metrics on three datasets improved by 1.08%, 0.93%, and 3.13%, respectively. This demonstrates that SA-MixNet can serve as a universal framework to extract more robust and intrinsic features by enhancing model invariance in varied scenes without additional supervision, showing its ability to significantly improve the performance of existing methods under data-constrained conditions. When applying SA-MixNet to complete DBNet, the performance is degraded compared to the case without edge detection branch, demonstrating that the proposed data-driven method can replace the additional supervision brought by the prior.

5. Conclusions

In this paper, we propose SA-MixNet, a novel framework for scribble-based road extraction from remote sensing images from a data-driven perspective, eliminating the requirements for additional priors. The proposed SA-Mixup

is an efficient scheme to construct samples with various complex scenes, and the invariance regularization significantly improves the generalization ability of the model by forcing it to behave consistent performance in complex and normal scenes and learning invariance feature of the targets.

References

- [1] R. Achanta, A. Shaji, K. Smith, A. Lucchi, P. Fua, and Sabine Süsstrunk. Slic superpixels compared to state-of-the-art superpixel methods. *IEEE Transactions on Pattern Analysis and Machine Intelligence*, page 2274–2282, 2012. [2](#), [3](#)
- [2] Wele Gedara Chaminda Bandara, Jeya Maria Jose Valanarasu, and Vishal M Patel. Spin road mapper: Extracting roads from aerial images via spatial and interaction space graph reasoning for autonomous driving. pages 343–350, 2022. [6](#)
- [3] A. Batra, S. Singh, G. Pang, S. Basu, and M. Paluri. Improved road connectivity by joint learning of orientation and segmentation. In *CVPR*, 2019. [6](#)
- [4] Ilke Demir, Krzysztof Koperski, David Lindenbaum, Guan Pang, Jing Huang, Saikat Basu, Forest Hughes, Devis Tuia, and Ramesh Raskar. Deepglobe 2018: A challenge to parse the earth through satellite images. In *2018 IEEE/CVF Conference on Computer Vision and Pattern Recognition Workshops (CVPRW)*, 2018. [6](#)
- [5] Ethan Harris, Antonia Marcu, Matthew Painter, Mahesan Niranjan, Adam Prügel-Bennett, and Jonathon Hare. Fmix: Enhancing mixed sample data augmentation. *arXiv preprint arXiv:2002.12047*, 2020. [3](#), [7](#)
- [6] S. Hong, S. Kwak, and B. Han. Weakly supervised learning with deep convolutional neural networks for semantic segmentation: Understanding semantic layout of images with minimum human supervision. *IEEE Signal Processing Magazine*, 34(6):39–49, 2017. [7](#)
- [7] Jang-Hyun Kim, Wonho Choo, and HyunOh Song. Puzzle mix: Exploiting saliency and local statistics for optimal mixup. *International Conference on Machine Learning*, 2020. [3](#), [7](#)
- [8] Jang-Hyun Kim, Wonho Choo, Hosan Jeong, and Hyun Oh Song. Co-mixup: Saliency guided joint mixup with supermodular diversity. *arXiv preprint arXiv:2102.03065*, 2021. [3](#), [7](#)
- [9] Samuli Laine and Timo Aila. Temporal ensembling for semi-supervised learning. *arXiv preprint arXiv:1610.02242*, 2016. [2](#)
- [10] Xingang Li, Yuebin Wang, Liqiang Zhang, Suhong Liu, Jie Mei, and Yang Li. Topology-enhanced urban road extraction via a geographic feature-enhanced network. *IEEE Transactions on Geoscience and Remote Sensing*, page 8819–8830, 2020. [1](#)
- [11] R. Lian and L. Huang. Weakly supervised road segmentation in high-resolution remote sensing images using point annotations. *IEEE Transactions on Geoscience and Remote Sensing*, PP(99):1–13, 2021. [1](#)
- [12] Di Lin, Jifeng Dai, Jiaya Jia, Kaiming He, and Jian Sun. Scribblesup: Scribble-supervised convolutional networks for semantic segmentation. pages 3159–3167, 2016. [7](#)
- [13] Jie Mei, Rou-Jing Li, Wang Gao, and Ming-Ming Cheng. Coanet: Connectivity attention network for road extraction from satellite imagery. *IEEE Transactions on Image Processing*, page 8540–8552, 2021. [1](#)
- [14] Volodymyr Mnih. Machine learning for aerial image labeling. 2013. [6](#)
- [15] Anton Obukhov, Stamatios Georgoulis, Dengxin Dai, and Luc Van Gool. Gated crf loss for weakly supervised semantic image segmentation. *arXiv preprint arXiv:1906.04651*, 2019. [2](#)
- [16] Yassine Ouali, Celine Hudelot, and Myriam Tami. Semi-supervised semantic segmentation with cross-consistency training. In *Proceedings of the IEEE/CVF Conference on Computer Vision and Pattern Recognition (CVPR)*, 2020. [2](#)
- [17] Junwen Pan, Pengfei Zhu, Kaihua Zhang, Bing Cao, Yu Wang, Dingwen Zhang, Junwei Han, and Qinghua Hu. Learning self-supervised low-rank network for single-stage weakly and semi-supervised semantic segmentation. *International Journal of Computer Vision*, 130(5):1181–1195, 2022. [2](#)
- [18] Antti Rasmus, Mathias Berglund, Mikko Honkala, Harri Valpola, and Tapani Raiko. Semi-supervised learning with ladder networks. *Advances in neural information processing systems*, 28, 2015. [2](#)
- [19] Mehdi Sajjadi, Mehran Javanmardi, and Tolga Tasdizen. Regularization with stochastic transformations and perturbations for deep semi-supervised learning, 2016. [2](#)
- [20] Ali Kemal Sinop and Leo Grady. A seeded image segmentation framework unifying graph cuts and random walker which yields a new algorithm. In *2007 IEEE 11th International Conference on Computer Vision*, 2007. [1](#)
- [21] Jihoon Tack, Sihyun Yu, Jongheon Jeong, Minseon Kim, Sung Ju Hwang, and Jinwoo Shin. Consistency regularization for adversarial robustness. *Proceedings of the AAAI Conference on Artificial Intelligence*, page 8414–8422, 2022. [2](#)
- [22] Meng Tang, Abdelaziz Djelouah, Federico Perazzi, Yuri Boykov, and Christopher Schroers. Normalized cut loss for weakly-supervised cnn segmentation. In *2018 IEEE/CVF Conference on Computer Vision and Pattern Recognition*, 2018. [2](#), [4](#)
- [23] S. Tao, Z. Chen, W. Yang, and W. Yin. Stacked u-nets with multi-output for road extraction. In *2018 IEEE/CVF Conference on Computer Vision and Pattern Recognition Workshops (CVPRW)*, 2018. [1](#)
- [24] Bin Wang, Guojun Qi, Sheng Tang, Tianzhu Zhang, Yunchao Wei, Linghui Li, and Yongdong Zhang. Boundary perception guidance: A scribble-supervised semantic segmentation approach. In *Proceedings of the Twenty-Eighth International Joint Conference on Artificial Intelligence*, 2019. [7](#), [1](#)
- [25] Y. Wei and S. Ji. Scribble-based weakly supervised deep learning for road surface extraction from remote sensing images. *IEEE Transactions on Geoscience and Remote Sensing*, (99), 2021. [1](#), [2](#), [3](#), [6](#), [8](#)

- [26] S. Wu, C. Du, H. Chen, Y. Xu, N. Guo, and N. Jing. Road extraction from very high resolution images using weakly labeled openstreetmap centerline. *International Journal of Geo-Information*, (11), 2019. 1, 2, 7
- [27] Bingrong Xu, Zhigang Zeng, Cheng Lian, and Zhengming Ding. Generative mixup networks for zero-shot learning. *IEEE Transactions on Neural Networks and Learning Systems*, page 1–12, 2022. 2
- [28] Sangdoo Yun, Dongyoon Han, Sanghyuk Chun, Seong Joon Oh, Youngjoon Yoo, and Junsuk Choe. Cutmix: Regularization strategy to train strong classifiers with localizable features. In *2019 IEEE/CVF International Conference on Computer Vision (ICCV)*, 2019. 3, 7
- [29] Hongyi Zhang, Moustapha Cisse, Yann N Dauphin, and David Lopez-Paz. mixup: Beyond empirical risk minimization. *arXiv preprint arXiv:1710.09412*, 2017. 2, 7
- [30] Jing Zhang, Xin Yu, Aixuan Li, Peipei Song, Bowen Liu, and Yuchao Dai. Weakly-supervised salient object detection via scribble annotations. In *2020 IEEE/CVF Conference on Computer Vision and Pattern Recognition (CVPR)*, 2020. 7
- [31] Ke Zhang and Xiahai Zhuang. Cyclemix: A holistic strategy for medical image segmentation from scribble supervision. In *Proceedings of the IEEE/CVF Conference on Computer Vision and Pattern Recognition (CVPR)*, pages 11656–11665, 2022. 2
- [32] Gaodian Zhou, Weitao Chen, Qianshan Gui, Xianju Li, and Lizhe Wang. Split depth-wise separable graph-convolution network for road extraction in complex environments from high-resolution remote-sensing images. *IEEE Transactions on Geoscience and Remote Sensing*, page 1–15, 2022. 1
- [33] L. Zhou, C. Zhang, and W. Ming. D-linknet: Linknet with pretrained encoder and dilated convolution for high resolution satellite imagery road extraction. In *2018 IEEE/CVF Conference on Computer Vision and Pattern Recognition Workshops (CVPRW)*, 2018. 6
- [34] Mingting Zhou, Haigang Sui, Shanxiong Chen, Junyi Liu, Weiyue Shi, and Xu Chen. Large-scale road extraction from high-resolution remote sensing images based on a weakly-supervised structural and orientational consistency constraint network. *ISPRS Journal of Photogrammetry and Remote Sensing*, 193:234–251, 2022. 1, 2
- [35] Jun-Yan Zhu, Taesung Park, Phillip Isola, and Alexei A. Efros. Unpaired image-to-image translation using cycle-consistent adversarial networks. In *2017 IEEE International Conference on Computer Vision (ICCV)*, 2017. 5

SA-MixNet: Structure-aware Mixup and Invariance Learning for Scribble-supervised Road Extraction in Remote Sensing Images

Supplementary Material

6. Rationale

6.1. Sensitivity Analysis of Regularization Weights

Loss Weight		DeepGlobe	
$\lambda_1(\mathcal{L}_{inv})$	$\lambda_2(\mathcal{L}_{C-D})$	IoU	F1
0	0	59.19	74.37
0.01	0.01	59.70	74.76
0.05	0.05	59.61	74.69
0.1	0.1	60.38	75.29
0.25	0.25	59.94	74.95
0.5	0.5	59.53	74.63
0.75	0.75	59.82	74.86
1	1	59.80	74.85

Table 5. Sensitivity analysis of loss weights on DeepGlobe dataset

Tab. 5 summarizes the obtained IoU and F1 scores by SA-MixNet on DeepGlobe dataset with different regularization weights. We denote the weights for \mathcal{L}_{inv} and \mathcal{L}_{C-D} as λ_1 and λ_2 , respectively. When λ_1 and λ_2 are both set to 0.01, there is a noticeable improvement in IoU and F1 scores against that without \mathcal{L}_{inv} and \mathcal{L}_{C-D} , *i.e.* $\lambda_1 = \lambda_2 = 0$. This indicates that the designed invariance regularization and connectivity regularization can effectively enhance the model’s performance. As the weight of regularization continues increasing, the model reaches its highest IoU and F1 scores at $\lambda_1 = 0.1$ and $\lambda_2 = 0.1$. While the weight of regularization is further increased, there may be a performance decline due to the potential trade-off effects on the base segmentation loss.

6.2. Generalizability Experiment

Method	BPG		BPG + SA-MixNet	
Dataset	IoU	F1	IoU	F1
DeepGlobe	54.00	70.13	59.01	74.22
Wuhan	50.86	67.43	54.19	70.29
Ma	55.45	71.34	60.62	75.49

Table 6. Generalizability experiment based on BPG

In Sec. 4.5, we discuss the framework’s generalizability by applying SA-MixNet on ScRoadExtractor’s DBNet [25] and present the performance on DeepGlobe, Wuhan,

and Massachusetts datasets in Tab. 4. To further validate the generalizability of the framework, our SA-MixNet, as a learning framework, is applied to BGP [24] and WeaklyOSM’s MD-ResUnet(MD) [26], and the proposed SC-label expansion, SA-Mixup and invariance-based regularization are integrated to them.

Tab. 6 presents the performance of applying SA-MixNet to BPG. The introduced new pseudo-labeling scheme and the learning framework lead to improvements of 5.01%, 3.33%, and 5.17% in the IoU performance metric on DeepGlobe, Wuhan and Massachusetts datasets, respectively.

Method	MD		MD + SA-MixNet	
Dataset	IoU	F1	IoU	F1
DeepGlobe	54.32	70.40	58.44	73.77
Wuhan	52.34	68.72	54.46	70.52
Ma	52.74	69.06	61.97	76.54

Table 7. Generalizability experiment based on MD-ResUnet

Similar performance improvements are also observed when applying SA-MixNet to MD-ResUnet. As shown in Tab. 7, there are performance gains of 4.12%, 2.12%, and 9.23% in the term of IoU scores on all selected datasets, respectively. Overall, the application of the proposed framework (SA-MixNet) to DBNet, BPG, and MD-ResUnet leads to significant performance improvements, regardless of whether additional supervision or priors are used by the original methods or not. This demonstrates the potential of our proposed framework to be generalized and applied to other methods, enhancing their performance by creating more diverse and complex samples, and forcing the models to behave invariantly on various scenes.